Article

pubs.acs.org/Biomac

Synthesis of Poly(meth)acrylates with Thioether and Tertiary Sulfonium Groups by ARGET ATRP and Their Use as siRNA Delivery Agents

Matthew C. Mackenzie,[†,§] Arun R. Shrivats,[‡,§] Dominik Konkolewicz,[†,∥] Saadyah E. Averick,[†] Michael C. McDermott,[‡] Jeffrey O. Hollinger,[‡] and Krzysztof Matyjaszewski*[,†]

[†]Department of Chemistry, Carnegie Mellon University, 4400 Fifth Avenue, Pittsburgh, Pennsylvania 15213, United States

[‡]Bone Tissue Engineering Center, Department of Biomedical Engineering, Carnegie Mellon University, Pittsburgh, Pennsylvania 15219, United States

Supporting Information

ABSTRACT: The field of RNA interference depends on the development of safe and efficient carriers for short interfering ribonucleic acid (siRNA) delivery. Conventional cationic monomers for siRNA delivery have utilized the nitrogen heteroatom to produce cationic charges. Here, we polymerized cationic sulfonium (meth)acrylate by activators regenerated by electron transfer (ARGET) atom transfer radical polymerization (ATRP) to form polymers with narrow molecular weight distributions for siRNA delivery. The tertiary sulfonium species was stable toward dealkylation in water but less stable in the polar aprotic solvent dimethyl sulfoxide. Block copolymers poly(ethylene oxide) with poly(meth)acrylate containing sulfonium moieties were prepared as an siRNA delivery platform. Results suggested block copolymers were biocompatible up to 50 μg/mL *in vitro* and formed polyplexes with siRNA. Additionally, block copolymers protected siRNAs against endonuclease digestion and facilitated knockdown of glyceraldehyde 3-phosphate dehydrogenase (*Gapdh*) mRNA expression in murine calvarial preosteoblasts. The versatility, biocompatibility, and cationic nature of these tertiary sulfonium groups are expected to find widespread biological applications.

INTRODUCTION

RNA interference (RNAi) is a promising therapeutic for post-transcriptional gene silencing with compelling potential for disease treatment.[1] The scope of RNAi also may include functioning as a probe for the elucidation of target gene function and pathogeneses.[2] However, the safe and efficient delivery of short interfering ribonucleic acids (siRNA) remains a barrier to success in either avenue. Challenges include toxicity associated with cationic delivery platforms, enzymatic degradation of siRNA, and electrostatic repulsion between siRNA and the anionic cell membrane surface.[3] Explicitly, siRNAs require delivery systems to provide protection from physiological degradation and to successfully navigate the *in vivo* environment.[4] Contemporary options for siRNA delivery, namely, viral vectors, present both immunological and safety concerns.[5] Additionally, difficulties associated with targeting specific cell phenotypes and limited siRNA loading capacities have necessitated the search for nonviral alternatives for siRNA delivery.[6]

Polymeric approaches for siRNA delivery are particularly promising for their superior versatility and ease of manipulation. The advent of reversible deactivation radical polymerization (RDRP) methods has facilitated the production of well-defined functional polymers for siRNA delivery.[7] Atom transfer radical polymerization (ATRP), in particular, is a versatile RDRP method that has been used to produce polymers for a wide range of applications, including siRNA delivery.[7−14] Recently, the use of chemical reducing agents to regenerate activator complexes have enabled the exploitation of low catalyst concentrations for ATRP.[11] One process, called activators regenerated by electron transfer (ARGET) ATRP, presents a green polymerization that requires minimal purification of final products.[15,16]

Traditional and ARGET ATRP have been used to prepare bioresponsive polymers with complex architectures.[7,17−21] For the purpose of gene delivery, polymers typically incorporate the nitrogen heteroatom to produce a cationic charge capable of binding anionic nucleic acids. However, the exploration of sulfur as an heteroatom alternative to nitrogen in cationic polymers has been minimal. Thioethers, and their alkylated tertiary sulfonium species, have been produced for several applications including gold extraction,[22] flocculants,[23] biomedical materials,[24] and functional substrates for polymer labeling.[25−27] To date, polymers containing thioether and tertiary sulfonium moieties have been prepared by ring-opening polymerization of *N*-carboxyanhydrides (NCA), reversible addition−fragmentation chain transfer (RAFT) polymerization, and free radical polymerization.[24,28−31] There has been one

Received: September 29, 2014
Revised: December 1, 2014
Published: December 17, 2014

report on direct polymerization of the tertiary sulfonium species by RDRP[29] and evaluation for siRNA delivery.[24] Recent efforts to repurpose the phosphonium ion for siRNA delivery further validate this approach.[32]

Here, we present conditions for the ATRP of acrylic and methacrylic monomers containing thioethers and their tertiary sulfonium derivatives. Specifically, we employed ARGET ATRP to create well-controlled polymers with relatively low concentrations of Cu catalyst.[15,16,33] The goal was the production of a new class of cationic polymers with applications for siRNA delivery. After refinement of the polymerization, we investigated the stability of the tertiary sulfonium species toward dealkylation with halide salts. To evaluate potential for siRNA delivery, we first determined dose-dependent cytotoxicity of block copolymers poly(ethylene oxide) (PEO) with poly(meth)acrylates containing the tertiary sulfonium species in murine calvarial preosteoblasts. Finally, we determined siRNA binding and dissociation characteristics of block copolymers and the siRNA delivery and gene knockdown capabilities in a proof-of-principle *in vitro* glyceraldehyde 3-phosphate dehydrogenase (*Gapdh*) model.

MATERIALS AND METHODS

Materials. Methacrylic acid (MAA, 99%, Aldrich) and acrylic acid (AA, 99%, Aldrich) were passed over a column of neutral alumina (Fisher Scientific) prior to use. 2-(Methylthio)ethanol (99%, Aldrich), 3-(ethyliminomethyleneamino)-*N*,*N*-dimethylpropan-1-amine hydrochloride (EDC-HCl, 99%, Carbosynth), 4-dimethylaminopyridine (DMAP, 99%, Aldrich), methyl trifluoromethansulfonate (MeOTf, 99%, Aldrich), ethyl α-bromoisobutyrate (EBiB, 98%, Aldrich), ethyl α-bromophenylacetate (EBPA, 98%, Aldrich), copper(II) bromide (99.999%, Aldrich), copper(II) chloride (99.999%, Aldrich), ascorbic acid (AscA, Sigma-Aldrich), acetone (ACS grade, Fisher Scientific), *N*,*N*-dimethylformamide (DMF, ACS grade, Fisher Scientific), methanol (MeOH, HPLC grade, Fisher Scientific), deuterated dimethyl sulfoxide (DMSO-d_6, 99.9%, Cambridge Isotope Laboratories), tetra-*n*-butylammonium bromide (TBA-Br, 98% Aldrich), tetra-*n*-butylammonium chloride (TBA-Cl, 98%, Aldrich), and anhydrous magnesium sulfate (99%, Aldrich) were used as received. Tris(pyridin-2-ylmethyl)amine (TPMA)[34] was prepared as previously reported in the literature.

Synthesis of DMS$^+$(M)A. MTEMA (253 mg, 1.58 mmol) [or (MTEA (242 mg, 1.65 mmol)] was dissolved in 20 mL of dry DCM in a tared 20 mL vial. This vial was cooled in an ice bath, and the contents were stirred. Then MeOTf (253 mg, 0.1691 mL, 1.54 mmol) [or (264.4 mg, 0.177 mL, 1.61 mmol)] was very slowly added to the vial. The vials were sealed and allowed to stir for 24 h. The solvent was removed, and then a strong vacuum was applied for a few hours to remove excess unreacted monomer. A high yield of very pure product was obtained, ~99%. t-MTEMA: ^{1}H NMR (δ, ppm, DMSO-d_6): 6.16 (s, 1H, =CH), 5.71 (s, 1H, =CH), 4.63 (t, 2H, CH2O), 3.85 (t, 2H, CH2S), 3.11 (s, 6H, (CH3)2S), 1.96 (s, 3H, CH3C). t-MTEA: ^{1}H NMR (δ, ppm, DMSO-d_6): 6.39−6.43 (dd, 1H, =CH), 6.22−6.27 (dd, 1H, =CH), 6.04−6.06 (dd, 1H, =CH), 4.57 (t, 2H, CH2O), 3.69 (t, 2H, CH2S), 2.95 (s, 6H, (CH3)2S). See Figure S3 and S4.

PEO$_{2k}$BPA-*b*-Poly(DSM$^+$MA) Synthesis Targeted Degrees of Polymerization DSM$^+$MA 15/35/45. MTEMA (1.0 g, 6.2 mmol), copper(II) chloride (0.6 mg, 0.004 mmol), TPMA (3.6 mg, 0.013 mmol), PEO$_{2k}$BPA (bromophenol acetate) (0.124 mg, 0.06 mmol), and acetone (1.0 mL) were added to a 10 mL Schlenk flask with a stir bar and degassed. 7.7 mg of ascorbic acid (degassed, 77 mg/mL in methanol) was added to the reaction, and the reaction mixture was heated at 35 °C for 24, 27, and 30 h. The polymer was purified by dialysis into acetone for 5 exchanges.

Polymer Alkylation Procedure. The block copolymer (50 mg) was alkylated by adding methyl triflate (94 mg, 0.57 mmol) in DCM (18 mL), and the reaction was stirred for 24 h and purified by dialysis into methanol and then aqueous 50 mM NaCl followed by ultrapure water and subsequently lyophilized. Three PEO$_{2k}$BPA-*b*-poly(DSM$^+$MA) block copolymers were prepared in this manner: M_n^{NMR} 5000, M_w/M_n^{GPC} of 1.17 PEO$_{2k}$BPA-*b*-poly(DSM$^+$MA$_{3k}$); M_n^{NMR} 9000, M_w/M_n^{GPC} of 1.56 PEO$_{2k}$BPA-*b*-poly(DSM$^+$MA$_{7k}$); M_n^{NMR} 11500, M_w/M_n^{GPC} of 1.48 PEO$_{2k}$BPA-*b*-poly(DSM$^+$MA)$_{12k}$ (Supporting Information, Table 1).

***Gapdh* Knockdown.** MC3T3-E1.4 cells were plated at a density of 50 000 cells/mL in 24-well tissue culture plates at 0.5 mL/well. After 24 h, RNAi treatments against *Gapdh* were prepared with PEO$_{2k}$BPA-*b*-poly(DSM$^+$MA)$_{12k}$ and delivered to cells at the polymer/siRNA weight ratios ranging from 10:1 to 100:1. Cell cultures were incubated for 24 h before the addition of siRNA treatments. Cells were lysed and analyzed by quantitative real-time polymerase chain reaction (qRT-PCR) using the CellsDirect one-step qRT-PCR kit (Invitrogen, Carlsbad, CA). Cell lysis, RNA extraction, and cDNA preparation were carried out according to the manufacturer's directions. All samples were analyzed for *ActB* and *Hmbs* gene expression in parallel with *Gapdh* expression. *Gapdh* expression was normalized to the geometric mean of *Actb* and *Hmbs* expression, using the comparative C_T method. Data were expressed as mean ± standard deviation of the relative gene expression fold change.

RESULTS AND DISCUSSION

Monomer Synthesis. The thioether monomers were prepared via 3-(ethyliminomethyleneamino)-*N*,*N*-dimethylpropan-1-amine (EDC) mediated coupling of 2-(methylthio)-ethanol with acrylic acid or methacrylic acid. The tertiary sulfonium-functionalized monomers were prepared by quantitative alkylation of the corresponding thioether using 1 equiv of methyl triflate (Scheme 1). ARGET ATRP conditions were

Scheme 1. Synthetic Route for the Preparation of Poly(DMS$^+$(M)A) by ARGET ATRP

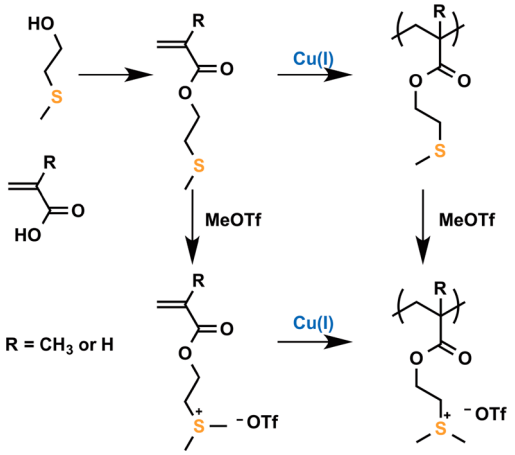

developed to prepare well-defined polymers from these monomers. Four monomers were investigated: a thioether or a tertiary sulfonium derivate containing either an acrylic or methacrylic polymerizable group. These monomers are referred to as 2-(methylthio)ethyl methacrylate (MTEMA), 2-(methylthio)ethyl acrylate (MTEA), dimethylsulfoniumethyl methacrylate (DMS$^+$MA), and dimethylsulfoniumethyl acrylate (DMS$^+$A).[28] Their structures are shown in Scheme 2, and the ^{1}H NMR spectra of these four monomers are given in Figures S1−S4.

Refinement of Polymerization Conditions. Polymerization conditions for each monomer were optimized until well-controlled polymers were prepared (i.e., M_w/M_n < 1.25). Initial conditions for the polymerization of the monomer MTEMA

Scheme 2. Structures of the Four Monomers Polymerized in This Study[a]

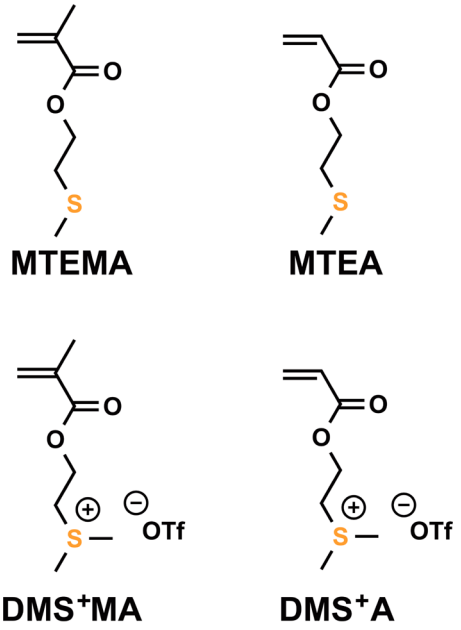

[a]Monomers are referred to as 2-(methylthio)ethyl methacrylate (MTEMA), 2-(methylthio)ethyl acrylate (MTEA), dimethyl sulfoniumethyl methacrylate (DMS$^+$MA), and dimethylsulfoniumethyl acrylate (DMS$^+$A).

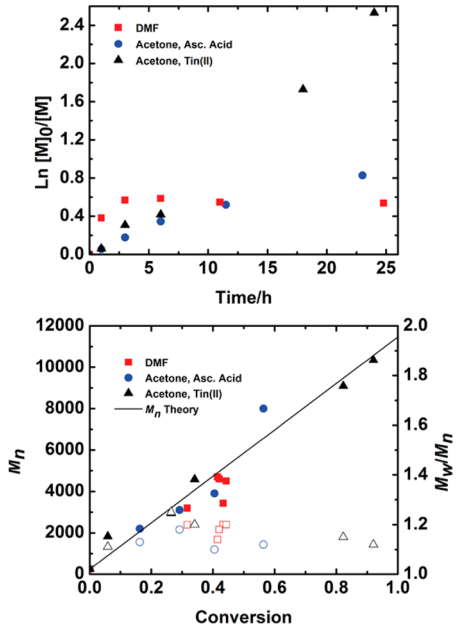

Figure 1. Kinetics of ARGET ATRP of MTEMA. (A) First-order kinetic plot and (B) M_n and M_w/M_n versus conversion plot. Red plot = [MTEMA]/[I]/[$CuBr_2$]/[TPMA]/[ascorbic acid] = 70:1:0.09:0.3:0.9, DMF 50% v/v, 60 °C, entry 1. Blue plot = [MTEMA]/[I]/[$CuCl_2$]/[TPMA]/[ascorbic acid] = 70:1:0.07:0.2:0.7, acetone 50% v/v, 35 °C, entry 4. Black plot = [MTEMA]/[I]/[$CuCl_2$]/[TPMA]/[tin(II) 2-ethylhexanoate] = 70:1:0.09:0.3:0.9, acetone 50% v/v, 35 °C, entry 7.

employed $CuBr_2$/TPMA as the catalyst in DMF (Table 1, entry 1) and ascorbic acid as the reducing agent. The reaction kinetics was nonlinear, and the experimental molecular weight was higher than the theoretical molecular weight (Figure 1). Consequently, a less polar aprotic solvent, acetone, was used to polymerize MTEMA.

Reactions in acetone were performed at a lower temperature (35 °C) than those in DMF (60 °C); these reactions also employed tin(II) 2-ethylhexanoate, rather than ascorbic acid, as the reducing agent (Table 1, entry 2). Reactions reached 90% conversion, with a narrow molecular weight distribution (M_w/M_n = 1.17) with good agreement between the theoretical and experimental M_n. A comparison between bromide and chloride Cu salts as reaction catalysts (Table 1, entries 2 and 3) produced similar rates (90 vs 91%, respectively) and control over molecular weight (M_w/M_n of 1.17 vs 1.12, respectively). Evaluation of tin(II) 2-ethylhexanoate and ascorbic acid as reducing agents (Table 1, entries 3 and 4) determined that both reducing agents resulted in a similar control over the molecular weight (M_w/M_n = 1.12). However, polymerization with ascorbic acid reached only 51% conversion after 24 h, whereas polymerization with tin(II) 2-ethylhexanoate achieved 91% conversion. Thus, the highest monomer conversions were achieved using an acetone solvent and tin(II) 2-ethylhexanoate reducing agent. GPC traces of the polymers synthesized using these conditions (Table 1, entry 4) are given in Figure S5.

Table 1. Experimental Conditions and Results for ARGET ATRP of MTEMA, MTEA, DMS$^+$MA, and DMS$^+$A[a]

reaction	[M]:[I]:[CuX_2]:[L]:[RA]	monomer	temp/°C	solvent	CuX_2	time/h	conv./%	$M_{n,th} \times 10^{-3}$	$M_n \times 10^{-3}$	M_w/M_n
1	70:1:0.09:0.3:0.9[b,h]	MTEMA	60	DMF	$CuBr_2$	24	42	4900	4700	1.14
2	50:1:0.07:0.2:0.7[c,g]	MTEMA	35	acetone	$CuBr_2$	24	90	7300	10 000	1.17
3	70:1:0.07:0.2:0.7[b,g]	MTEMA	35	acetone	$CuCl_2$	24	91	10 500	13 000	1.12
4	70:1:0.07:0.2:0.7[b,h]	MTEMA	35	acetone	$CuCl_2$	24	51	6000	8300	1.12
5	70:1:0.07:0.2:0.7[d,h]	MTEA	60	DMF	$CuBr_2$	24	58	6100	9900	1.54
6	50:1:0.07:0.2:0.7[e,g]	MTEA	35	acetone	$CuBr_2$	24	26	2400	2500	1.09
7	70:1:0.07:0.2:0.7[e,g]	MTEA	45	acetone	$CuBr_2$	24	27	3000	3600	1.08
8	100:1:0.09:0.3:0.9[f,h]	MTEA	35	acetone	$CuBr_2$	33	19	2300	4500	1.06
9	50:1:0.09:0.3:0.9[b,h]	DMS$^+$MA	50	MeOH	$CuBr_2$	24	99	15 000	20 000	1.32
10	70:1:0.09:0.3:0.9[c,h]	DMS$^+$MA	50	MeOH	$CuCl_2$	23	89	11 000	6600	1.22
11	70:1:0.09:0.3:0.9[d,h]	DMS$^+$A	50	MeOH	$CuCl_2$	23	73	8300	7400	1.19

[a]40% [M] (v/v). [b][I] = [ethyl α-bromophenylacetate] = 45 mM. [c][I] = [ethyl α-bromophenylacetate] = 61 mM. [d][I] =[ethyl 2-bromoisobutyrate] = 49 mM. [e][I] = [ethyl 2-bromoisobutyrate] = 67 mM. [f][I] = [ethyl 2-bromoisobutyrate] = 52 mM. [g]Reducing agent = tin(II) 2-ethylhexanoate. [h]Reducing agent = ascorbic acid. The apparent molecular weights of the thioether polymers were estimated using linear poly(methyl methacrylate) standards (neutral polymers) with THF as the eluent and poly(ethylene oxide) standards (tertiary sulfonium polymers) with H_2O as the eluent.

dx.doi.org/10.1021/bm501449a | Biomacromolecules 2015, 16, 236−245

Polymerizations conducted in acetone, in contrast to DMF, consistently provided linear first-order kinetic plots, suggesting a constant radical concentration and preservation of chain end functionality. Similar refinements in protocol were conducted for polymerization of the thioether containing acrylate monomer, MTEA (Figure 2). First, $CuBr_2$/TPMA in DMF

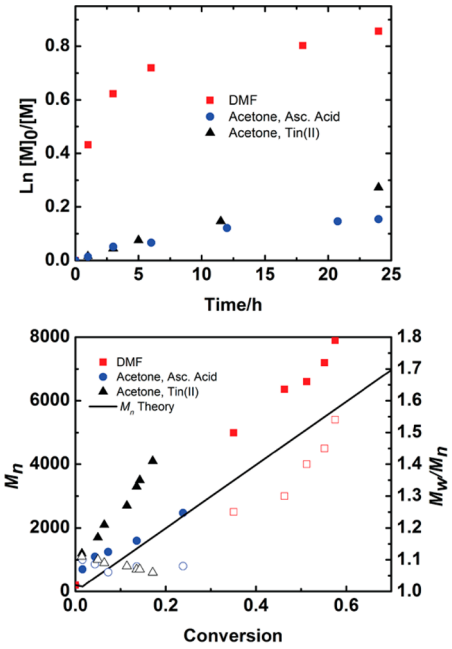

Figure 2. Kinetics of ARGET ATRP of MTEA. (A) First-order kinetics plot and (B) M_n and M_w/M_n versus conversion plot. Red plot = [MTEA]/[I]/[$CuBr_2$]/[TPMA]/[ascorbic acid] = 70:1:0.07:0.2:0.7, DMF 50% v/v, 60 °C, entry 5. Blue plot = [MTEA]/[I]/[$CuBr_2$]/[TPMA]/[ascorbic acid] = 100:1:0.09:0.3:0.9, acetone 50% v/v, 35 °C, entry 8. Black plot = [MTEA]/[I]/[$CuBr_2$]/[TPMA]/[tin(II) 2-ethylhexanoate] = 70:1:0.07:0.2:0.7, acetone 50% v/v, 35 °C, entry 7.

was used to polymerize MTEA, with ascorbic acid as the reducing agent (Table 1, entry 5). As seen in the polymerization of MTEMA, the conversion stopped at 55% at 6 h. Molecular weight distributions were broad (M_w/M_n >1.5); moreover, reaction kinetics were nonlinear, suggesting a significant loss of chain end functionality through the polymerization.

Polymerizations in acetone as the solvent and tin(II) ethylhexanoate as the reducing agent (Table 1, entry 6) resulted in polymers with narrow molecular weight distributions (M_w/M_n = 1.09) and M_n values that grew linearly with conversion. However, conversion peaked at 26% after 24 h. Variations in polymerization temperatures and alternate reducing agents (Table 1, entries 6–8) had no significant impact on conversion, control over the molecular weight, or the molecular weight distribution. Polymerizations in acetone produced linear semilogarithmic kinetic plots and M_w/M_n values between 1.05 and 1.1. The GPC traces of the polymers synthesized using the conditions in Table 1, entry 8, are given in Figure S6.

As an alternative to the polymerization of monomers with thioether moieties, we directly polymerized the monomers with tertiary sulfonium groups by ARGET ATRP. Initial polymerizations were conducted in methanol with $CuBr_2$/tris(pyridin-2-ylmethyl)amine (TPMA) as the catalyst and ascorbic acid as the reducing agent (Table 1, entry 9). These conditions yielded 99% conversion in 24 h (approximately 50% after 2 h), although they gave a relatively broad molecular weight distribution (M_w/M_n = 1.32). Polymerizations with $CuCl_2$/TPMA as the catalyst (Table 1, entry 10) produced a slower reaction, reaching 89% in 24 h; molecular weight distributions were narrow, with M_w/M_n = 1.22. These conditions were also employed for DMS$^+$A, yielding well-defined polymers with 73% conversion and M_w/M_n = 1.19 (Table 1, entry 11).

In summary, polymerization conditions for the thioether methacrylate (MTEMA) used $CuCl_2$/TPMA as the catalytic system with acetone as the solvent at 35 °C (Table 1, entries 3 and 4). A rate of polymerization was increased when tin(II) ethylhexanoate was used as the reducing agent as compared to that with ascorbic acid. A well-controlled polymerization of thioether acrylate (MTEA) was observed in acetone with $CuBr_2$/TPMA as the catalytic system (Table 1, entries 6–8). The polymerization of monomers with tertiary sulfonium groups, DMS$^+$MA and DMS$^+$A (Figure 3), by ARGET ATRP

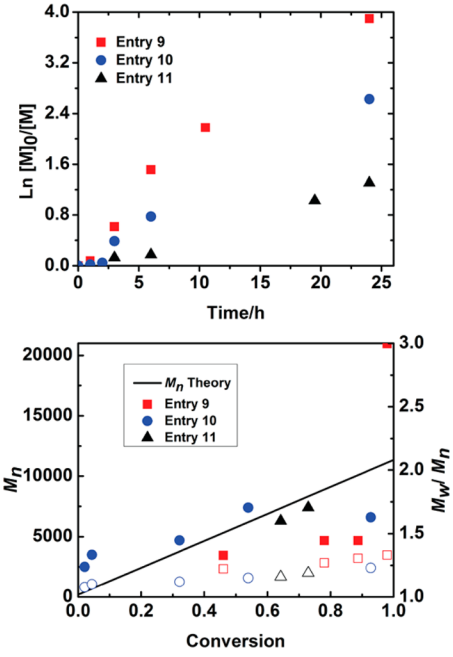

Figure 3. Kinetics of ARGET ATRP of DMS$^+$MA and DMS$^+$A. (A) First-order kinetic plot and (B) M_n and M_w/M_n versus conversion plot. Red plot = [DMS$^+$MA]/[I]/[$CuBr_2$]/[TPMA]/[ascorbic acid] = 50:1:0.09:0.3:0.9, MeOH 50% v/v, 50 °C, entry 9. Blue plot = [DMS$^+$MA]/[I]/[$CuCl_2$]/[TPMA]/[ascorbic acid] = 70:1:0.09:0.3:0.9, MeOH 50% v/v, 50 °C, entry 10. Black plot = [DMS$^+$A]/[I]/[$CuCl_2$]/[TPMA]/[ascorbic acid] = 70:1:0.09:0.3:0.9, MeOH 50% v/v, 50 °C, entry 11.

resulted in high conversions and narrow molecular weight distributions (M_w/M_n < 1.25) using the catalytic system of $CuCl_2$/TPMA in MeOH and ascorbic acid as the reducing agent (Table 1, entries 10 and 11).

Stability of Tertiary Sulfonium Species. Thioether compounds (based on MTEMA and MTEA) were quantitatively converted to tertiary sulfonium species by reaction with methyl triflate. However, tertiary sulfonium ions may be dealkylated in the presence of more nucleophilic halide anions.[35,36] This was previously reported for polymers with benzylic sulfonium species.[29] In biological media, the concentration of halide ions is greater 100 mM and thus the dealkylation of the tertiary sulfonium species is an important

dx.doi.org/10.1021/bm501449a | Biomacromolecules 2015, 16, 236–245

parameter for use in biological applications.[37,38] Thus, we investigated the dealkylation rates of a representative monomer, DMS^+A, in varying concentration of halide ions in a polar organic solvent, dimethyl sulfoxide (DMSO). Initial conditions were a 1:5 molar ratio of DMS^+A to bromide (Br^-) or chloride (Cl^-) ions ($[DMS^+A]_0$ = 0.0236 M), and the decrease of the tertiary sulfonium groups was monitored over time by NMR (Figures S7 and S8). The disappearance of the tertiary sulfonium groups coincided with the appearance of thioether groups and methyl bromide, indicating that halide anions slowly dealkylated the tertiary sulfonium groups. After 96 h of reaction time, ~22% of the sulfonium species were dealkylated by the chloride anion and ~19% of the sulfonium species were dealkylated by the bromide anion (Figure 4). Although there

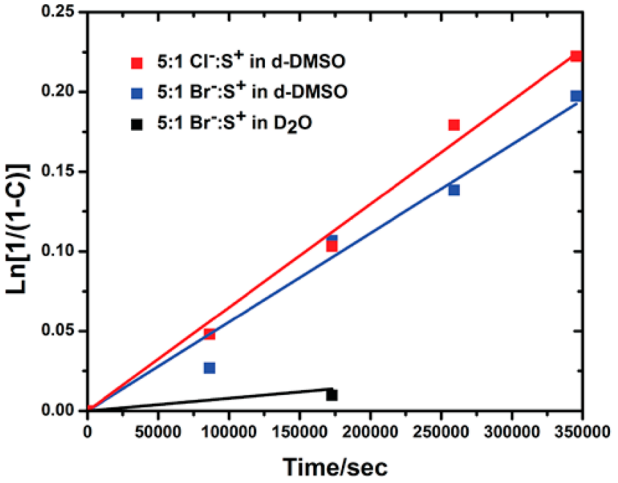

Figure 4. Comparison of halide and solvent for dealkylation of tertiary sulfonium containing monomer (DMS^+A) in either *d*-DMSO or D_2O. $[DMS^+A]_0$ = 0.0236 M and $[\text{halide ion}]_0$ = 0.118 M at room temperature.

was notable dealkylation of the DMS^+A, a minimal difference was detected between the rate of dealkylation by chloride and bromide anions. Table 2 provides an estimated rate coefficient for dealkylation and the half-life of the sulfonium species in *d*-DMSO under physiological conditions of 120 mM of halide salts.

Table 2. Stability of Tertiary Sulfonium Monomer and Polymer with Bromide and Chloride in DMSO and Water[a]

reaction	k (M^{-1} s^{-1})	$t_{1/2}$ (days)	solvent
S^+:Br^-	5.0×10^{-6}	~13	DMSO
S^+:Cl^-	5.6×10^{-6}	~11	DMSO
S^+:Br^-	$<6 \times 10^{-7}$	>100	D_2O

[a]The rate coefficients for dealkylation were determined, $[DMS^+A]_0$ = 0.0236 M and $[\text{halide ion}]_0$ = 0.118 M at room temperature, and the $t_{1/2}$ was determined from the rate coefficient, assuming a concentration of halide = 120 mM (as is typical under biological conditions).

To provide more fidelity to the aqueous *in vivo* environment, the dealkylation of the sulfonium species was determined in water. Unlike the DMSO system where data suggested a ~10% dealkylation after 48 h, the aqueous environment produced less than 2% dealkylation after 48 h in a 5-fold molar excess of halide/DMS^+A ($[DMS^+A]_0$ = 0.0236 M) (Figures S9 and S10). An upper bound on the dealkylation rate coefficient in aqueous media is given in Table 2, as well as a lower bound on the half-life of sulfonium species under biological conditions of halide ion concentration of 120 mM. Results indicated that the tertiary sulfonium species was stable in aqueous media, even in the presence of high concentrations of halide anions. The increased stability of the sulfonium ions in water may be due to the stabilizing effect of the polar aqueous environment on the sulfonium species; this stabilizing effect would not be provided by the organic solvent, DMSO.

The dealkylation of the tertiary sulfonium was investigated with respect to halide ion concentration (in excess of DMS^+A). The molar ratio of DMS^+A to bromide anions was varied from a 1:2.5 to 1:10 ($[DMS^+A]_0$ = 0.0236 M) in *d*-DMSO (Figure 5). In *d*-DMSO, the rate of the dealkylation of DMS^+A was

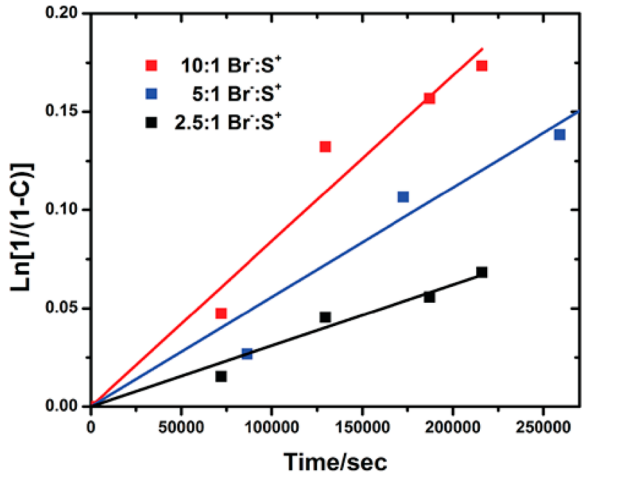

Figure 5. Comparison of several concentrations of bromide in *d*-DMSO and effect on rate of dealkylation. $[DMS^+A]_0$ = 0.0236 M and $[Br^-]_0$ = 0.059−0.236 M at room temperature.

proportional to the concentration of the halide anion, indicating that dealkylation in DMSO was first-order in halide and second-order overall. The average dealkylation rate coefficient of DMS^+A was determined to be $5 \pm 1 \times 10^{-6}$ M^{-1} s^{-1}.

The dealkylation of the tertiary sulfonium monomers was followed by an investigation of their polymer counterparts using ^1H NMR. Typical NMR spectra for the dealkylation of poly(DMS^+A) by both bromide and chloride anions in DMSO are provided in the Supporting Information (Figures S11 and S12). However, in the presence of increasing nucleophile amounts, an increase in reaction rate was not observed, unlike in the case of the monomer (Figure 6). At several concentrations of nucleophile, the final conversion of tertiary sulfonium to thioether was ~20% after 72 h. Interestingly, when concentrations of the halide anion were increased, there was no commensurate increase in the rate of the dealkylation of the polymer, shown in Figure 5.

The dealkylation rate of the polymer demonstrated no dependence on halide concentration, within the studied concentrations. This was unexpected due to monomer dealkylation exhibiting first-order kinetics with respect to halide concentration and second-order kinetics overall. Furthermore, the rate of monomer dealkylation with 5 equiv of bromide to sulfonium was almost 50% slower than the corresponding polymer dealkylation rate of the polymer. This suggests that a local polyelectrolyte effect may be responsible for the increased

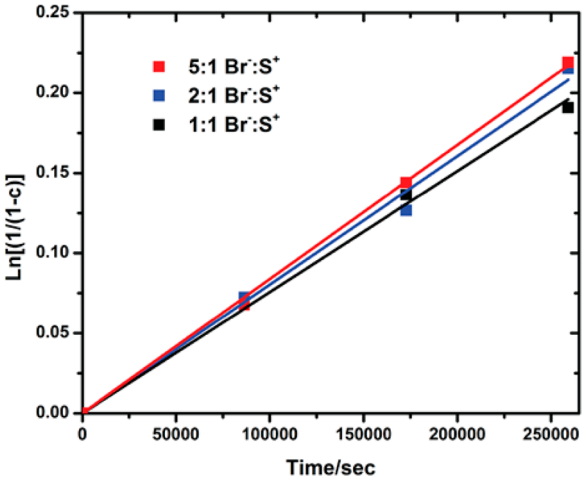

Figure 6. Comparison of rate of dealkylation with increasing concentration of bromide in *d*-DMSO. $[pDMS^+A]_0$ = 0.0236 M (concentration of sulfonium groups) and $[Br^-]_0$ = 0.0236−0.118 M at room temperature.

rate of polymer dealkylation and its weak dependence on halide concentration. In D_2O, there was negligible dealkylation of poly(DMS$^+$A) in D_2O with an excess of bromide anions (Figures S13 and S14). These results demonstrate the stability of the tertiary sulfonium species in biologically relevant concentrations of halide anions.

Preparation of Block Copolymers for siRNA Delivery. To reduce toxicity due to the cationic nature of the tertiary sulfonium species, block copolymers combining DMS$^+$MA and poly(ethylene oxide) 2-bromophenylacetate (PEO_{2k}BPA, M_n = 2000) were prepared by ARGET ATRP. DMS$^+$MA was selected for its structural similarity to dimethylaminoethyl methacrylate (DMAEMA), a cationic monomer based on the nitrogen heteroatom that is frequently studied for siRNA delivery.[39] DMS$^+$MA molecular weights of 3000, 7000 and 12 000 were used to produce polymers, termed PEO_{2k}BPA-*b*-poly(DMS$^+$MA)$_n$. The DMS$^+$MA segments with varying lengths were synthesized to examine the effect of increasing the polymer size and cationic content on siRNA delivery. Detailed characterization data is given in Table S1.

Biocompatibility of PEO_{2k}BPA-*b*-Poly(DMS$^+$MA). A crucial criterion for gene delivery is carrier biocompatibility, which we define as the absence of cytotoxicity. Dose-dependent cytotoxicity in murine calvarial preosteoblasts (MC3T3s) was evaluated after 24 and 48 h periods by live/dead staining. After 24 h in culture, there was no evidence of cytotoxicity due to PEO_{2k}BPA-*b*-poly(DMS$^+$MA)$_{3k/7k/12k}$ doses of 50 and 100 μg/mL (Figure S13). After 48 h, cell cultures continued to indicate viability, although there was a decrease in cell proliferation at doses of 100 μg/mL PEO_{2k}BPA-*b*-poly(DMS$^+$MA)$_{7k}$ and PEO_{2k}BPA-*b*-poly(DMS$^+$MA)$_{12k}$ block copolymers (Figure 7). This retardation of cell proliferation was not observed in cultures treated with PEO_{2k}BPA-*b*-poly(DMS$^+$MA)$_{3k}$.

To provide a quantitative comparison of cytotoxicity, MTS-based viability assessments were conducted after 48 h in culture (Figure 8). Results suggest that doses greater than 100 μg/mL of PEO_{2k}BPA-*b*-poly(DMS$^+$MA)$_{7k}$ and PEO_{2k}BPA-*b*-poly(DMS$^+$MA)$_{12k}$ polymers reduced cell viability by roughly 20%. While this decrease in relative cell viability was statistically significant, the degree of reduction was significantly less than that for known cytotoxic polymer polyethylenimine $(PEI)_{25k}$ (p < 0.05). The results suggest that PEO_{2k}BPA-*b*-poly(DMS$^+$MA)$_{7k}$ and PEO_{2k}BPA-*b*-poly(DMS$^+$MA)$_{12k}$ polymers inhibit cellular proliferation rather than cause cellular death. Furthermore, at a dose of 50 μg/mL (per 50 000 cells), cell viability with all three block copolymers remained within tolerance of 100%. Notably, cell cultures treated with PEO_{2k}BPA-*b*-poly(DMS$^+$MA)$_{3k}$ block copolymers remained at greater than 95% cell viability up to doses of 400 μg/mL.

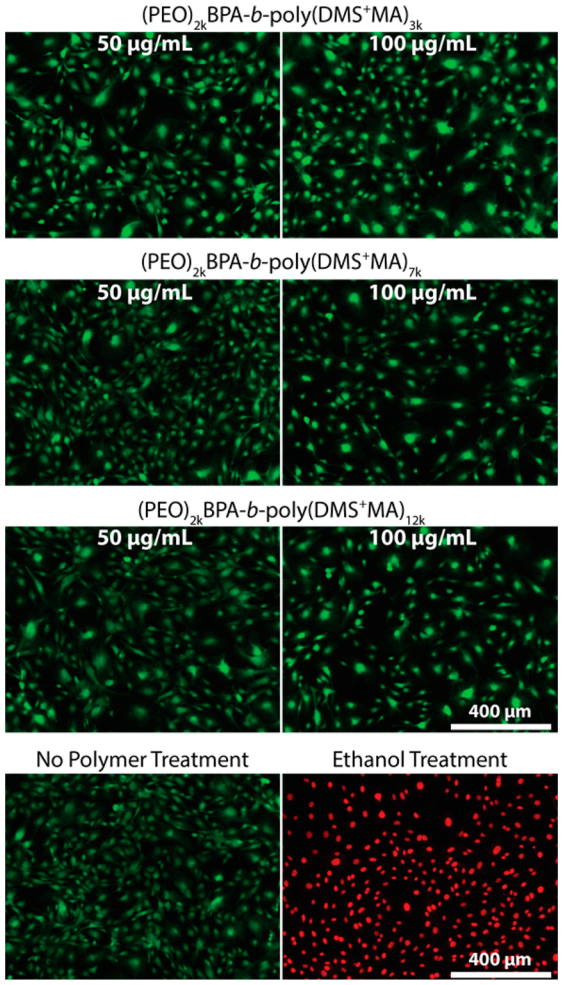

Figure 7. Live/dead staining of MC3T3 cells 48 h after treatment by PEO_{2k}BPA-*b*-poly(DMS$^+$MA)$_{3k/7k/12k}$ block copolymers. DMS$^+$MA chain lengths are 3k (first row), 7k (second row), and 12k (third row). As determined by the predominant fluorescent calcein (green), major cytotoxicity is not a consequence of block copolymer delivery at 50 and 100 μg/mL. 100 μg/mL treatments produced visible reductions in cell density, indicating that polymer delivery may impede cell proliferation, although it is not necessarily inducing cell death.

The inhibition of cell proliferation was further investigated over a 10 day period using PicoGreen-based quantification of cellular DNA content (Figure 9). Results indicated that statistically significant reductions in cell viability and proliferation occurred in cultures treated with PEO_{2k}BPA-*b*-poly(DMS$^+$MA)$_{12k}$ block copolymers at a dose of 200 μg/mL. PEO_{2k}BPA-*b*-poly(DMS$^+$MA)$_{12k}$ doses of 50 and 100 μg/mL resulted in only marginal reductions in viability after 4, 7, and 10 days in culture. All treatments with PEO_{2k}BPA-*b*-poly(DMS$^+$MA)$_{3k}$ and PEO_{2k}BPA-*b*-poly(DMS$^+$MA)$_{7k}$ produced insignificant effects on cell viability over the 10 day experiment.

dx.doi.org/10.1021/bm501449a | *Biomacromolecules* 2015, 16, 236−245

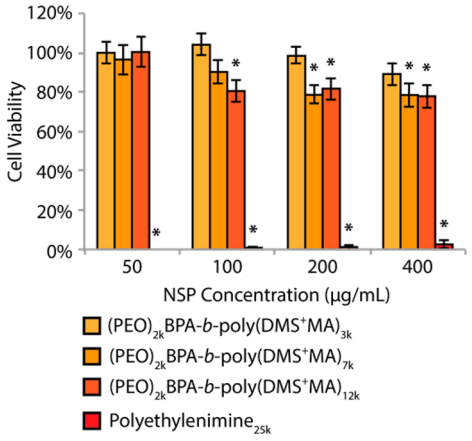

Figure 8. MTS-based cell viability after 48 h in culture. PEO_{2k}BPA-*b*-poly$(DMS^+MA)_{7k}$ polymers reduce cell viability at doses greater than 200 μ/mL, whereas PEO_{2k}BPA-*b*-poly$(DMS^+MA)_{12k}$ polymers reduce viability at doses greater than 100 μg/mL. All block copolymer variants produced no significant changes to cell viability at a dose of 50 μg/mL.

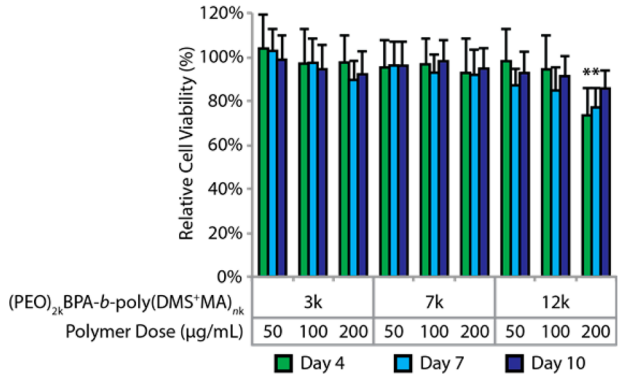

Figure 9. PicoGreen-based cellular viability after 4, 7, and 10 days in culture. PEO_{2k}BPA-*b*-poly$(DMS^+MA)_{12k}$ polymers delivered at 200 μg/mL induce significant reductions in cell viability over 10 days in culture. PEO_{2k}BPA-*b*-poly$(DMS^+MA)_{3k}$ and PEO_{2k}BPA-*b*-poly-$(DMS^+MA)_{7k}$ polymers demonstrated no significant reduction in relative cell viability over 4, 7, and 10 days in culture.

siRNA Complexation Properties of PEO_{2k}BPA-*b*-Poly-(DMS^+MA). The mechanism that governs cationic polymer–siRNA binding is proposed to rely on electrostatic interactions.[4] An analysis of polymer–siRNA complexation by agarose gel electrophoresis determined the ability of PEO_{2k}BPA-*b*-poly-(DMS^+MA) block copolymers to form complexes (termed polyplexes) with siRNA (Figure 10). PEO_{2k}BPA-*b*-poly-$(DMS^+MA)_{3k}$ blocks produced complexation occurring at polymer/siRNA weight ratios of 500:1. PEO_{2k}BPA-*b*-poly-$(DMS^+MA)_{7k}$ and PEO_{2k}BPA-*b*-poly$(DMS^+MA)_{12k}$ polymers demonstrated notable improvement in siRNA binding ability, with complexation occurring at 25:1 and 10:1 ratios, respectively (Figure 10B,C). Analyses of siRNA complexation typically provide an approximation of polymer/siRNA ratios that may efficiently deliver siRNAs. As such, the approximate quantities of PEO_{2k}BPA-*b*-poly$(DMS^+MA)_{3k}$ block copolymer required to deliver a fixed dose of siRNA would be more than 10 times greater than what can be achieved using PEO_{2k}BPA-*b*-poly$(DMS^+MA)_{7k}$ or PEO_{2k}BPA-*b*-poly$(DMS^+MA)_{12k}$ as siRNA carriers. However, efficient delivery may also require easy decomplexation, as shown for star-like polymers and nanogels with cationic ammonium species.[40,41]

Nuclease Resistance of Polyplexes. Analyses of PEO_{2k}BPA-*b*-poly$(DMS^+MA)_{7k}$ and PEO_{2k}BPA-*b*-poly-$(DMS^+MA)_{12k}$ block copolymers were continued by examining siRNA protection capabilities and dissociation characteristics. There are several endogenous mechanisms to prevent exogenous genetic material from entering target cells;[4] successful gene delivery platforms require the ability to prevent enzyme-induced degradation of siRNAs. The polymer property to inhibit enzyme-induced degradation by steric hindrance was determined by incubating PEO_{2k}BPA-*b*-poly$(DMS^+MA)_{7k}$ and PEO_{2k}BPA-*b*-poly$(DMS^+MA)_{12k}$ polyplexes with RNase A, a potent endonuclease, prior to loading in agarose gels. siRNA staining intensity (quantified by ImageJ gel analysis) correlates with increasing siRNA protection. Gel visualization suggested that PEO_{2k}BPA-*b*-poly$(DMS^+MA)_{7k}$ blocks provided protection for siRNAs, although siRNA band intensity was reduced 78 ± 11% after incubation with RNase A. Unbound siRNAs were completely degraded after incubation with RNase A. PEO_{2k}BPA-*b*-poly$(DMS^+MA)_{12k}$ polyplexes, however, reduced siRNA intensity by 7 ± 6%. The differences in siRNA protection between PEO_{2k}BPA-*b*-poly$(DMS^+MA)_{7k}$ and PEO_{2k}BPA-*b*-poly$(DMS^+MA)_{12k}$ were statistically significant ($p < 0.01$) (Student's *t* test).

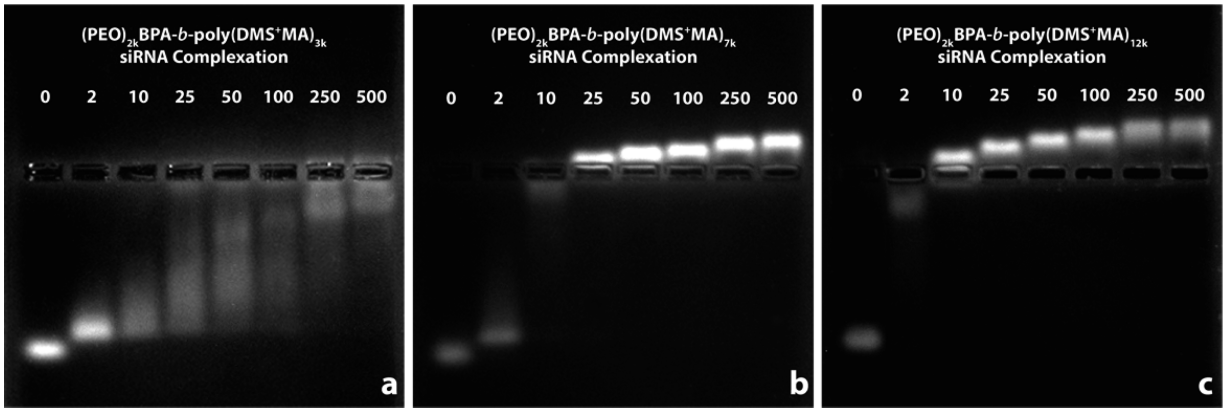

Figure 10. siRNA complexation analysis by agarose gel electrophoresis of PEO_{2k}BPA-*b*-poly$(DMS^+MA)_{3k}$ (a), PEO_{2k}BPA-*b*-poly$(DMS^+MA)_{7k}$ (b), and PEO_{2k}BPA-*b*-poly$(DMS^+MA)_{12k}$ (c) polymers. PEO_{2k}BPA-*b*-poly$(DMS^+MA)_{3k}$ appears to fully complex at polymer/siRNA weight ratios greater than 500:1 (listed above each well). PEO_{2k}BPA-*b*-poly$(DMS^+MA)_{7k}$ complexes fully with siRNAs at 25:1, whereas PEO_{2k}BPA-*b*-poly$(DMS^+MA)_{12k}$ polymers complex with siRNAs at 10:1 weight ratios.

dx.doi.org/10.1021/bm501449a | *Biomacromolecules* 2015, 16, 236–245

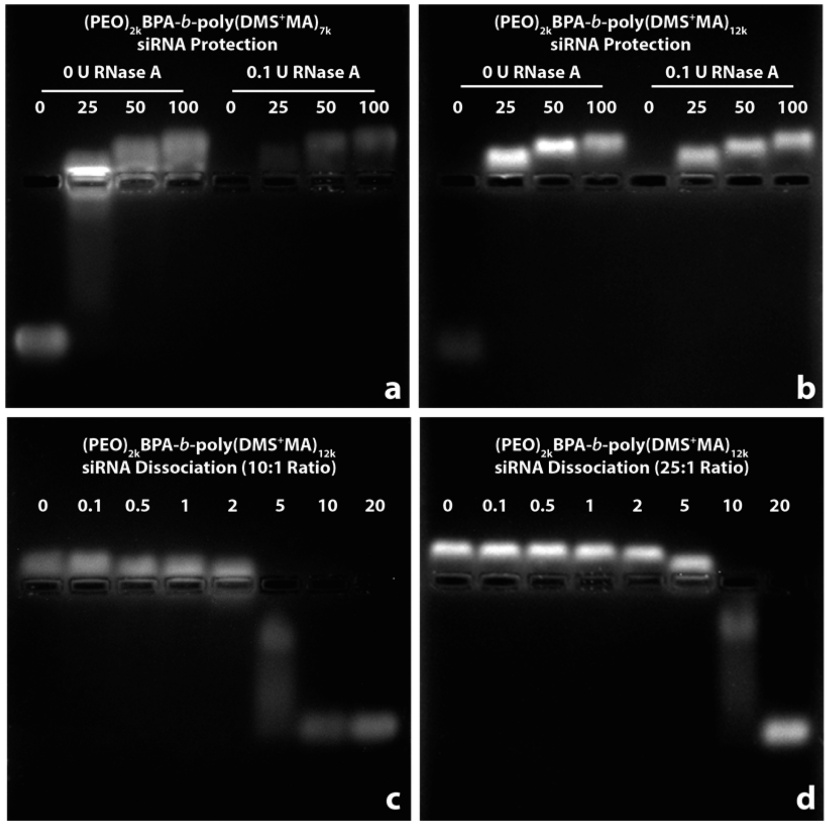

Figure 11. Top: Gel electrophoresis analysis of siRNA protection of PEO_{2k}BPA-*b*-poly$(DMS^+MA)_{7k}$ (a) and PEO_{2k}BPA-*b*-poly$(DMS^+MA)_{12k}$ (b) polymers. PEO_{2k}BPA-*b*-poly$(DMS^+MA)_{7k}$ polyplexes demonstrate significant reductions in siRNA staining intensity in the presence of 0.1U RNase A; however, reductions in PEO_{2k}BPA-*b*-poly$(DMS^+MA)_{12k}$ polyplexes are not as marked. Bottom: An analysis of siRNA dissociation was performed at 10:1 PEO_{2k}BPA-*b*-poly$(DMS^+MA)_{12k}$/siRNA ratios (c) and 25:1 PEO_{2k}BPA-*b*-poly$(DMS^+MA)_{12k}$/siRNA ratios (d). The siRNA release profile of both polymer/siRNA ratios in the presence of heparan sulfate vary, indicating that the dissociation point of polymers and siRNA may be tuned by varying the polymer/siRNA ratio.

Disassociation of Polyplexes by Heparan Sulfate. PEO_{2k}BPA-*b*-poly$(DMS^+MA)_{12k}$ blocks were the candidate material for the determination of dissociation characteristics with bound siRNA. The rationale for this selection was based on the strength of siRNA binding and protection imparted by the PEO_{2k}BPA-*b*-poly$(DMS^+MA)_{12k}$ blocks. The putative mechanism for the release of siRNA *in vivo* is by substitution of siRNAs by polyanions. The property of PEO_{2k}BPA-*b*-poly$(DMS^+MA)_{12k}$ polyplexes was determined by gel electrophoresis; after complexation, heparan sulfate (a polyanion) was added to complexes for 30 min before loading into agarose gels (Figure 11C,D). The amount of heparan sulfate added was varied ratiometrically with respect to siRNA. At constant PEO_{2k}BPA-*b*-poly$(DMS^+MA)_{12k}$/siRNA ratios of 10:1 and 25:1 (Figure 11, panels C and D, respectively), the heparan sulfate/siRNA ratios in each well were varied from 0.1:1 to 20:1, respectively. The left-most sample in each gel was a control group with no heparan sulfate.

In 10:1 polyplexes (Figure 11C), siRNA dissociation from the PEO_{2k}BPA-*b*-poly$(DMS^+MA)_{12k}$ polymer began at 5:1 heparan sulfate/siRNA ratios. In 25:1 polyplexes (Figure 11D), dissociation of the siRNA from polyplexes occurred at a ratio of 10:1 heparan sulfate/siRNA. This data indicates an increasing binding affinity between PEO_{2k}BPA-*b*-poly$(DMS^+MA)_{12k}$ and siRNAs at higher polymer/siRNA ratios. Furthermore, the outcome suggests that the dissociation of siRNA from polyplexes may be tuned by varying polymer/siRNA ratios. Successful siRNA delivery must achieve a balance of siRNA binding affinity to provide siRNA protection and release siRNAs in the cytoplasm. The varying dissociation patterns with 10:1 and 25:1 PEO_{2k}BPA-*b*-poly$(DMS^+MA)_{12k}$/siRNA weight ratios validates that dissociation occurs more readily at lower polymer/siRNA ratios. Furthermore, our previous conclusion that siRNA protection increases as polymer/siRNA ratios increase requires an analysis of polymer/siRNA ratios for target gene knockdown.

***Gapdh* Knockdown.** PEO_{2k}BPA-*b*-poly$(DMS^+MA)_{12k}$ block copolymers were further characterized for gene knockdown. An analysis of target gene knockdown was performed by probing glyceraldehyde 3-phosphate dehydrogenase (*Gapdh*) expression in murine calvarial preosteoblasts cultured in 10% serum. Delivery of *Gapdh* siRNA at varying polymer/siRNA ratios resulted in significant reductions in *Gapdh* mRNA expression, determined by quantitative real-time polymerase chain reaction (qRT-PCR; Figure 12). PEO_{2k}BPA-*b*-poly$(DMS^+MA)_{12k}$/siRNA ratios from 25:1 to 100:1 resulted in significant reductions in *Gapdh* expression. In this range, *Gapdh* mRNA levels were reduced from 55.57 ± 14.17% to 59.46 ± 14.86% and were deemed to be statistically significant ($p < 0.05$). This ∼40−45% knockdown was produced in a highly transcribed housekeeping gene, illustrating the potency of the RNAi treatment. Polymer/siRNA ratios of 10:1 did not result in significant knockdown, indicating that the siRNA protection of this polyplex RNAi treatment may have been insufficient in a serum-containing environment. Alternatively, reductions in surface charge of polyplexes may have reduced internalization

dx.doi.org/10.1021/bm501449a | *Biomacromolecules* 2015, 16, 236−245

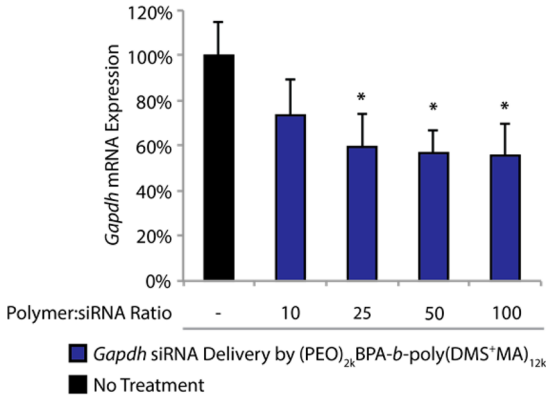

Figure 12. *Gapdh* mRNA expression by quantitative real-time PCR in MC3T3 cells 48 h after RNAi treatment by PEO_{2k}BPA-*b*-poly-$(DMS^+MA)_{12k}$ to deliver *Gapdh* siRNAs. PEO_{2k}BPA-*b*-poly-$(DMS^+MA)_{12k}$/siRNA ratios greater than 25:1 (D25) demonstrate significant reductions in *Gapdh* mRNA.

efficiency, thus hindering target gene knockdown. Regardless, results suggest that siRNA delivery and subsequent gene knockdown may be achieved in mammalian culture systems containing serum by the preparation of PEO_{2k}BPA-*b*-poly-$(DMS^+MA)_{12k}$ block copolymers.

CONCLUSIONS

The field of polymer-mediated siRNA delivery has relied mainly upon the nitrogen heteroatoms (alkyl amines) to form the cationic backbone of sophisticated polymer architectures. Here, we report the direct synthesis of cationic polymers containing tertiary sulfonium species by ARGET ATRP for siRNA complexation and delivery. Synthetic conditions were developed to polymerize both acrylic and methacrylic monomers, containing either the thioether group or the tertiary sulfonium group. The optimized conditions resulted in linear first-order polymerization kinetics, linear evolution of molecular weight with conversion, and polymers with narrow molecular weight distributions. Aqueous media, analogous to *in vitro* and *in vivo* biological environments, produced negligible dealkylation of the sulfonium group in the presence of halide ions; the estimated half-life of the sulfonium species was greater than 3 months. It was determined that DMS^+MA monomers, when synthesized into block copolymers with PEO_{2k}, may have applications for siRNA delivery. Biocompatibility analyses demonstrated that 50 μg/mL doses (per 50 000 cells) have no measured toxic effects on the mammalian cell viability up to 10 days in culture. PEO_{2k}BPA-*b*-poly$(DMS^+MA)_{nk}$ block copolymers and siRNAs formed complexes and thus inhibited enzymatic degradation of bound siRNAs in the presence of endonucleases. Furthermore, the release of siRNA from polyplexes is tunable by varying polymer/siRNA ratios. Finally, target-specific gene knockdown was validated in a *Gapdh* serum-containing culture model where PEO_{2k}BPA-*b*-poly-$(DMS^+MA)_{12k}$ block copolymers achieved roughly 45% reductions in *Gapdh* mRNA after 48 h. The success of DMS^+MA-based polymers in siRNA delivery applications opens the door for the evaluation of a wide variety of cationic polymers based on the sulfur heteroatom. The relatively mild reaction conditions of ARGET ATRP along with the polymer biocompatibility demonstrated here are strong indicators for this class of polymer use in biological environments.

ASSOCIATED CONTENT

Supporting Information

Detailed instrumentation, synthesis of monomers, general methods for ARGET ATRP of MTEMA and MTEA, methods for dealkylation studies. Further information on biological experimentation and resultant data (i.e., confocal microscope images and GAPDH mRNA expression after siRNA delivery with commercially available vectors). ^{1}H NMR of monomers and polymers and dealkylation studies. This material is available free of charge via the Internet at http://pubs.acs.org.

AUTHOR INFORMATION

Corresponding Author

*E-mail: km3b@andrew.cmu.edu. Phone: (412) 268-3209.

Present Address

[‖](D.K.) Department of Chemistry and Biochemistry, Miami University, 651 East High Street, Oxford, Ohio 45056, United States.

Author Contributions

[§]M.C.M. and A.R.S. contributed equally to this work.

Notes

The authors declare no competing financial interest.

ACKNOWLEDGMENTS

The authors acknowledge Antonina Simakova and Jon Wilcox for insightful discussions, Hironobu Murata for use of aqueous GPC, Dr. Gayathri C. Withers for assistance with NMR measurements, and NMR instrumentation at CMU was partially supported by NSF (CHE-1039870). This work was partially supported by NSF (CHE 1400052) and DMRDP (DoD) grant W81XWH1120073.

ABBREVIATIONS

ATRP, atom transfer radical polymerization; ARGET, activators regenerated by electron transfer; PEO, poly(ethylene oxide); MTEMA, 2-(methylthio)ethyl methacrylate; MTEA, 2-(methylthio)ethyl acrylate; DMS^+MA, dimethylsulfoniumethyl methacrylate; DMS^+A, dimethylsulfoniumethyl acrylate; DMSO, dimethyl sulfoxide

REFERENCES

(1) Burnett, J. C.; Rossi, J. J.; Tiemann, K. Current progress of siRNA/shRNA therapeutics in clinical trials. *Biotechnol. J.* **2011**, *6*, 1130−46.

(2) Liu, J.; Carmell, M. A.; Rivas, F. V.; Marsden, C. G.; Thomson, J. M.; Song, J. J.; Hammond, S. M.; Joshua-Tor, L.; Hannon, G. J. Argonaute2 is the catalytic engine of mammalian RNAi. *Science* **2004**, *305*, 1437−41.

(3) Whitehead, K. A.; Langer, R.; Anderson, D. G. Knocking down barriers: advances in siRNA delivery. *Nat. Rev. Drug. Discovery* **2009**, *8*, 129−38.

(4) Wang, J.; Lu, Z.; Wientjes, M. G.; Au, J. L. Delivery of siRNA therapeutics: barriers and carriers. *AAPS J.* **2010**, *12*, 492−503.

(5) Woods, N. B.; Bottero, V.; Schmidt, M.; von Kalle, C.; Verma, I. M. Gene therapy: therapeutic gene causing lymphoma. *Nature* **2006**, *440*, 1123.

(6) Tomanin, R.; Scarpa, M. Why do we need new gene therapy viral vectors? Characteristics, limitations and future perspectives of viral vector transduction. *Curr. Gene. Ther.* **2004**, *4*, 357−72.

(7) Matyjaszewski, K. Atom transfer radical polymerization (ATRP): current status and future perspectives. *Macromolecules* **2012**, *45*, 4015−39.

(8) Matyjaszewski, K.; Xia, J. H. Atom transfer radical polymerization. *J. Polym. Sci., Part A: Polym. Chem.* **2001**, *101*, 2921−90.

(9) Wang, J. S.; Matyjaszewski, K. Controlled/"living" radical polymerization. Atom transfer radical polymerization in the presence of transition-metal complexes. *J. Am. Chem. Soc.* **1995**, *117*, 5614−5.
(10) Matyjaszewski, K.; Patten, T. E.; Xia, J. H. Controlled/"living" radical polymerization. Kinetics of the homogeneous atom transfer radical polymerization of styrene. *J. Am. Chem. Soc.* **1997**, *119*, 674−80.
(11) Tsarevsky, N. V.; Matyjaszewski, K. "Green" atom transfer radical polymerization: from process design to preparation of well-defined environmentally friendly polymeric materials. *Chem. Rev.* **2007**, *107*, 2270−99.
(12) di Lena, F.; Matyjaszewski, K. Transition metal catalysts for controlled radical polymerization. *Prog. Polym. Sci.* **2010**, *35*, 959−1021.
(13) Kamigaito, M.; Ando, T.; Sawamoto, M. Metal-catalyzed living radical polymerization. *Chem. Rev.* **2001**, *101*, 3689.
(14) Matyjaszewski, K.; Tsarevsky, N. V. Macromolecular engineering by atom transfer radical polymerization. *J. Am. Chem. Soc.* **2014**, *136*, 6513−33.
(15) Jakubowski, W.; Matyjaszewski, K. Activators regenerated by electron transfer for atom-transfer radical polymerization of (meth)acrylates and related block copolymers. *Angew. Chem., Int. Ed.* **2006**, *118*, 4594−8.
(16) Matyjaszewski, K.; Jakubowski, W.; Min, K.; Tang, W.; Huang, J.; Braunecker, W. A.; Tsarevsky, N. V. Polymerization Special Feature: Diminishing catalyst concentration in atom transfer radical polymerization with reducing agents. *Proc. Natl. Acad. Sci. U.S.A.* **2006**, *103*, 15309−14.
(17) Pyun, J.; Matyjaszewski, K. Synthesis of nanocomposite organic/inorganic hybrid materials using controlled/"living" radical polymerization. *Chem. Mater.* **2001**, *13*, 3436−48.
(18) Oh, J. K.; Drumright, R.; Siegwart, D. J.; Matyjaszewski, K. The development of microgels/nanogels for drug delivery applications. *Prog. Polym. Sci.* **2008**, *33*, 448−77.
(19) Gao, H. F.; Matyjaszewski, K. Synthesis of functional polymers with controlled architecture by CRP of monomers in the presence of cross-linkers: from stars to gels. *Prog. Polym. Sci.* **2009**, *34*, 317−50.
(20) Sheiko, S. S.; Sumerlin, B. S.; Matyjaszewski, K. Cylindrical molecular brushes: synthesis, characterization, and properties. *Prog. Polym. Sci.* **2008**, *33*, 759−85.
(21) Lee, H. I.; Pietrasik, J.; Sheiko, S. S.; Matyjaszewski, K. Stimuli-responsive molecular brushes. *Prog. Polym. Sci.* **2010**, *35*, 24−44.
(22) Hemvasdukij, S.; Ngeontae, W.; Imyim, A. Sulfur containing poly(*N*-isopropylacrylamide) copolymer hydrogels for thermosensitive extraction of gold(III) ions. *J. Appl. Polym. Sci.* **2011**, *120*, 3098−108.
(23) Bailey, F. E.; La Combe, E. M. Synthesis and some properties of some sulfonium polyelectrolytes: polymers and copolymers derived from methylthioethyl acrylate. *J. Macromol. Sci., Part A: Pure Appl. Chem.* **1970**, *4*, 1293−300.
(24) Hemp, S. T.; Allen, M. H.; Smith, A. E.; Long, T. E. Synthesis and properties of sulfonium polyelectrolytes for biological applications. *ACS Macro Lett.* **2013**, 731−5.
(25) Marra, K. G.; Kidani, D. D. A.; Chaikof, E. L. Cytomimetic Biomaterials. 2. In-situ polymerization of phospholipids on a polymer surface. *Langmuir* **1997**, *13*, 5697−701.
(26) Hoover, M. F. Cationic quaternary polyelectrolytes—a literature review. *J. Macromol. Sci., Part A: Pure Appl. Chem.* **1970**, *4*, 1327−1418.
(27) Li, Y.; Ouyang, J. Characterization of polymer-supported rare-earth metal complexes and their catalytic behavior in polymerization of conjugated dienes. *J. Macromol. Sci., Part A: Pure Appl. Chem.* **1987**, *24*, 227−42.
(28) Kramer, J. R.; Deming, T. J. Preparation of multifunctional and multireactive polypeptides via methionine alkylation. *Biomacromolecules* **2012**, *13*, 1719−23.
(29) Borguet, Y. P.; Tsarevsky, N. V. Controlled radical polymerization of a styrenic sulfonium monomer and post-polymerization modifications. *Polym. Chem.* **2013**, *4*, 2115.
(30) Ohashi, T.; Hayashi, Y.; Oda, R. Syntheses of Poly- (2-methylsulfinyl-ethyl) methacrylate and poly-(2-methylsulfonyl-ethyl) methacrylate. *Kobunshi Kagaku* **1967**, *24*, 334−6.
(31) Hatch, M. J.; Meyer, F. J.; Lloyd, W. D. Sulfonium polymers derived from Ar-vinylbenzyl chloride. I. Exploratory study of the preparation and properties of the monomers and polymers. *J. Appl. Polym. Sci.* **1969**, *13*, 721−44.
(32) Ornelas-Megiatto, C.; Wich, P. R.; Frechet, J. M. Polyphosphonium polymers for siRNA delivery: an efficient and nontoxic alternative to polyammonium carriers. *J. Am. Chem. Soc.* **2012**, *134*, 1902−5.
(33) Braunecker, W. A.; Matyjaszewski, K. Controlled/living radical polymerization: features, developments, and perspectives. *Prog. Polym. Sci.* **2007**, *32*, 93−146.
(34) Tyeklar, Z.; Jacobson, R. R.; Wei, N.; Murthy, N. N.; Zubieta, J.; Karlin, K. D. Reversible-reaction of dioxygen (and carbon monoxide) with a copper(I) complex. X-ray structures of relevant mononuclear Cu(I) precursor adducts and the trans-(mu-1,2-peroxo)dicopper(II) product. *J. Am. Chem. Soc.* **1993**, *115*, 2677−89.
(35) Belkin, Y. V.; Polezhaeva, N. A.; Arbuzov, B. A. Dealkylation of 2-methylphenyl sulfuranylidendimedone with tertiary arsines. *Russ. Chem. Bull.* **1977**, *26*, 2012.
(36) Haryono, A.; Yamamoto, K.; Shouji, E.; Tsuchida, E. Synthesis and nucleophilic dealkylation of poly[alkyl-(4-(phenylthio)phenyl)-sulfonium trifluoromethanesulfonate]s. *Macromolecules* **1998**, *31*, 1202−7.
(37) Forrester, J.; Jones, R. V. H.; Newton, L.; Preston, P. N. Synthesis and reactivity of benzylic sulfonium salts: benzylation of phenol and thiophenol under near-neutral conditions. *Tetrahedron* **2001**, *57*, 2871−84.
(38) Rothgeb, T. M.; Jones, B. N.; Hayes, D. F.; Gurd, R. S. Coordination complexes and catalytic properties of proteins and related substances. 87. Methylation of glucagon, characterization of the sulfonium derivative, and regeneration of the native covalent structure. *Biochemistry* **1977**, *16*, 5813−8.
(39) Convertine, A. J.; Benoit, D. S.; Duvall, C. L.; Hoffman, A. S.; Stayton, P. S. Development of a novel endosomolytic diblock copolymer for siRNA delivery. *J. Controlled Release* **2009**, *133*, 221−9.
(40) Cho, H. Y.; Averick, S. E.; Paredes, E.; Wegner, K.; Averick, A.; Jurga, S.; Das, S. R.; Matyjaszewski, K. Star polymers with a cationic core prepared by ATRP for cellular nucleic acids delivery. *Biomacromolecules* **2013**, *14*, 1262−7.
(41) Averick, S. E.; Paredes, E.; Irastorza, A.; Shrivats, A. R.; Srinivasan, A.; Siegwart, D. J.; Magenau, A. J.; Cho, H. Y.; Hsu, E.; Averick, A. A.; Kim, J.; Liu, S.; Hollinger, J. O.; Das, S. R.; Matyjaszewski, K. Preparation of cationic nanogels for nucleic acid delivery. *Biomacromolecules* **2012**, *13*, 3445−9.